

MUSE 3D spectroscopy of BA-type supergiants in NGC 300

Gemma González-Torà^{1,2,3}, Miguel A. Urbaneja³, Norbert Przybilla³,
Stefan Dreizler⁴, Martin M. Roth⁵, Sebastian Kamann², and
Norberto Castro⁵

¹European Southern Observatory (ESO), Karl-Schwarzschild-Str. 2, 85748 Garching bei München, Germany

²Astrophysics Research Institute, LJMU, 146 Brownlow Hill, Liverpool L3 5RF, UK

³Institut für Astro- und Teilchenphysik, Universität Innsbruck, Technikerstr. 25/8, 6020 Innsbruck, Austria

⁴Institute for Astrophysics, University of Göttingen, Friedrich-Hund-Platz 1, 37077 Göttingen, Germany

⁵Leibniz-Institut für Astrophysik (AIP), An der Sternwarte 16, 14482 Postdam, Germany

Abstract. We present the results obtained using spectroscopic data taken with the intermediate-resolution Multi Unit Spectroscopic Explorer (MUSE) of B and A-type supergiants and bright giants in the Sculptor Group galaxy NGC 300. For our analysis, a hybrid local thermodynamic equilibrium (LTE) line-blanketing+non-LTE method was used to improve the previously published results for the same data. In addition, we present some further applications of this work, which includes extending the flux-weighted gravity luminosity relationship (FGLR), a distance determination method for supergiants. This pioneering work opens up a new window to explore this relation, and also demonstrates the enormous potential of integral field spectroscopy (IFS) for extragalactic quantitative stellar studies.

Keywords. Galaxies: individual (NGC 300) – Galaxies: distances and redshifts – Stars: early-type – Stars: fundamental parameters – supergiants

1. Introduction

Resolving individual stars in other galaxies has been a turning point for astronomy (e.g., Hubble 1929; Baade 1944). The best candidates for such observations are massive BA-type supergiants, as they are the brightest objects in optical light, reaching absolute visual magnitudes of $M_V \simeq -9.5$ (e.g. Humphreys & Davidson 1979; Humphreys & Aaronson 1987). The spiral galaxy NGC 300 is located at the Sculptor Group, close to the Galactic southern pole. These galaxies are the least affected by Galactic extinction and therefore convenient targets to study. Moreover, NGC 300 is oriented face-on, being a great candidate for quantitative multi-object slit spectroscopy (e.g., Bresolin et al. 2002, 2004; Urbaneja et al. 2005). An extremely powerful tool for this purpose is the so-called integral field spectroscopy (IFS). This technique allows for a spectrum for each pixel across an image to be obtained simultaneously. The Multi Unit Spectroscopic Explorer (MUSE, Bacon et al. 2014) on the European Southern Observatory Very Large Telescope (ESO VLT) is groundbreaking in this context, as it combines a wide field of view with high spatial sampling. Spectroscopic analysis of the brightest objects in nearby galaxies, i.e. supergiant stars, can be performed to determine their stellar parameters.

The present study based on González-Torà et al. (2022) provides a detailed analysis of MUSE spectra of BA-type supergiants and bright giants in NGC 300 in the field seen in

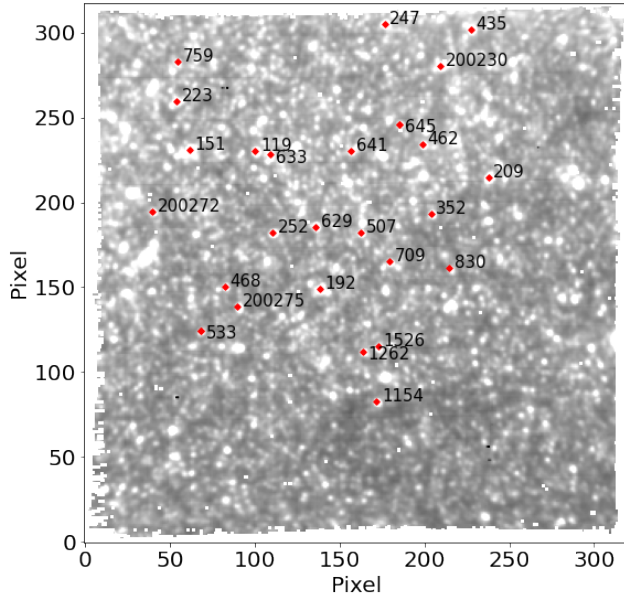


Figure 1: Chart of NGC 300 field (i) in spaxel coordinates with the programme stars marked in red and their ID numbers marked in black (according to Paper I).

Figure 1 from (Roth et al. 2018, henceforth Paper I). The analysis is based on synthetic spectra accounting for deviations from local thermodynamic equilibrium (LTE).

2. Methods

The spectroscopic data were obtained using MUSE (Bacon et al. 2014), in the wide field mode (WFM) with $1' \times 1'$ spatial coverage and $0.2''$ sampling. The pointing observed under the best seeing conditions ($\text{FWHM} = 0.47''\text{--}0.59''$, measured from the data) was investigated.

The initial reduction was achieved with the MUSE pipeline V1.0 (see Paper I for details Weilbacher et al. 2020). The final data were produced in the form of a datacube, and the spectra of 606 individual sources were extracted using the PampelMUSE software (Kamann et al. 2013).

Out of these 606 extracted sources, 26 were classified as late-B to early-A supergiants or bright giants in Paper I with a $7 < \text{S/N} \lesssim 20$, the minimum was demanded for our analysis to provide valid results. They are identified in Fig. 1. Due to model restrictions, we ended up with 16 objects that fulfilled the criteria for a quantitative analysis (see González-Torà et al. 2022, for more details).

We consider a grid of model atmospheres covering the parameter space defined by the effective temperature T_{eff} and surface gravity $\log g$. We adopt the modelling methodology by Przybilla et al. (2006) for the analysis of our final sample of 16 stars. Very briefly, the method employs a combination of model atmosphere structures calculated under the assumption of LTE+line-blanketing and a detailed non-LTE level population as well

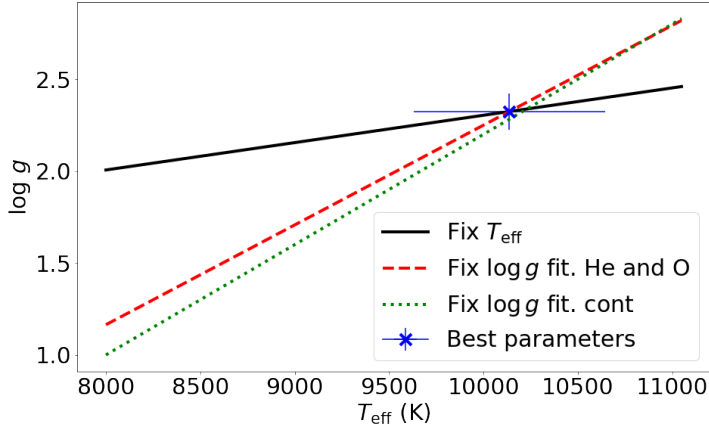


Figure 2: Example of the method used to determine the temperature and surface gravity for star #151. The solid black line shows the locus obtained by varying $\log g$ (in cgs units) for each fixed model-grid T_{eff} fitting the hydrogen lines. As red-dashed and green-dotted lines, we show the loci obtained by varying T_{eff} at each fixed model-grid $\log g$ best fitting the He I and O I lines, and the metal-line dominated 4950-5600 Å region, respectively. The blue cross marks the intersection of the loci, corresponding with the adopted atmospheric parameter values.

as line-formation calculations. The reader is referred to Przybilla et al. (2006) for the advantages and drawbacks of this hybrid approach, as well as its limitations.

We followed a well-established methodology to find the best solution for each object. First, by adopting T_{eff} , we found the model that best reproduces the features sensitive to gravity changes (the hydrogen Balmer lines); this step was repeated for different adopted T_{eff} values, hence allowing us to define the locus of models for which the Balmer lines are equally well represented. This is referred as the $\log g$ locus. Similarly, but adopting the surface gravity, we identified the model that best reproduces the T_{eff} sensitive features (in our case either the metal lines He I and O I lines, or the metal-line dominated 4950-5600 Å region). We repeated this step for different values of $\log g$, defining the T_{eff} locus. Finally, the intersection of both lines represents the best possible solution for a given object in the $T_{\text{eff}}-\log g$ plane (see Fig. 2).

A catalogue of Johnson B - and V -band magnitudes for sources in NGC 300, based on the work by Pietrzyński et al. (2001), was kindly provided by F. Bresolin (private communication). It allowed to calculate bolometric magnitudes M_{bol} from the extinction-corrected apparent V -band magnitudes, the distance to NGC 300 of $d = 1.86 \pm 0.07$ Mpc as determined by Rizzi et al. (2006), and the bolometric corrections ($B.C.$) for each object individually, calculated from tailored models.

3. The flux-weighted gravity luminosity relationship (FGLR)

The FGLR was first derived by Kudritzki et al. (2003) as a new method for distance determination of supergiants:

$$-M_{\text{bol}} = a(\log g_{\text{F}} - 1.5) + b \quad (3.1)$$

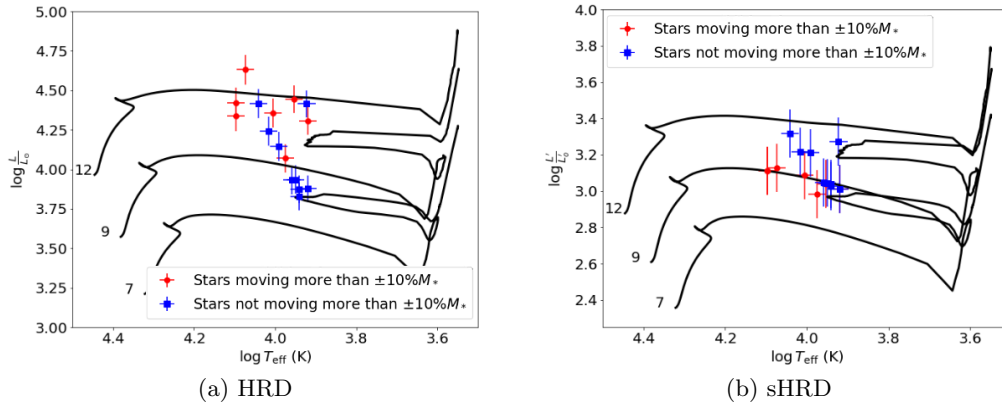


Figure 3: a) HRD with evolutionary tracks for different masses (black solid lines, in M_{\odot}) accounting for rotation (Ekström et al. 2012). The red dots represent sample stars that move by more than 10% their evolutionary mass track position with respect to the sHRD in Fig. 3b, and the blue squares are those that move less than 10%. b) Same as Fig. 3a, but for the sHRD. The L' is defined as the inverse of the flux-weighted gravity.

with a determined by the mass-luminosity relation ($L \propto M^x$) exponent x to $a = 2.5x/(1-x)$, and g_F the so-called flux-weighted gravity, defined as $g_F = g \times (T_{\text{eff}}/10^4)^{-4}$.

This relation holds for all supergiants and bright giants that have a constant luminosity track when they move to the right of the Hertzsprung-Russell diagram (HRD). Therefore, this relation can be used to estimate the bolometric magnitudes, luminosities, and distances of supergiants and bright giants for which only spectral information is available. If we are able to resolve massive stars in distant galaxies, this can be a very powerful tool to determine extragalactic distances.

To study the FGLR, the stars need to be at the correct evolutionary stage. To verify that, we plotted the stars in relation to evolutionary tracks from Ekström et al. (2012) in the regular HRD (Fig. 3a) and compared their position with respect to the same tracks in the sHRD (Fig. 3b). The sHRD (Langer & Kudritzki 2014) shows L' which is the inverse of g_F , with respect to T_{eff} . Using the sHRD, we can place the stars with only their spectroscopic information and without any knowledge of their distance or brightness. The advantage of the sHRD is that the stars fall into different iso-gravity lines, enabling to discriminate stars with different radii as well as multiple systems.

The red dots in Figs. 3a and 3b represent stars that move more than the 10% threshold (corresponding to their mass error), which indicates that they are not well-behaved objects. These stars show significantly larger spectroscopic than evolutionary masses that are derived from comparison with evolutionary tracks. The blue squares in Figs. 3a and 3b do not move by more than the threshold, and we can assume a good correspondence between their spectral information and their true evolutionary stage and their single star status. The latter stars are certain to be in the supergiant stage and therefore the FGLR would hold.

To prove our last point, we considered our 16 stars along with the objects previously studied by Kudritzki et al. (2008) to derive the FLGR. As we can see in Fig. 4, the blue squares follow the old FGLR within their error limits. The initial FGLR gives the old parameters determined by Kudritzki et al. (2008): $a_{\text{old}} = -3.52$ and $b_{\text{old}} = 8.11$. Adding the contribution of our newly found supergiants (blue squares in Fig. 4), we obtained

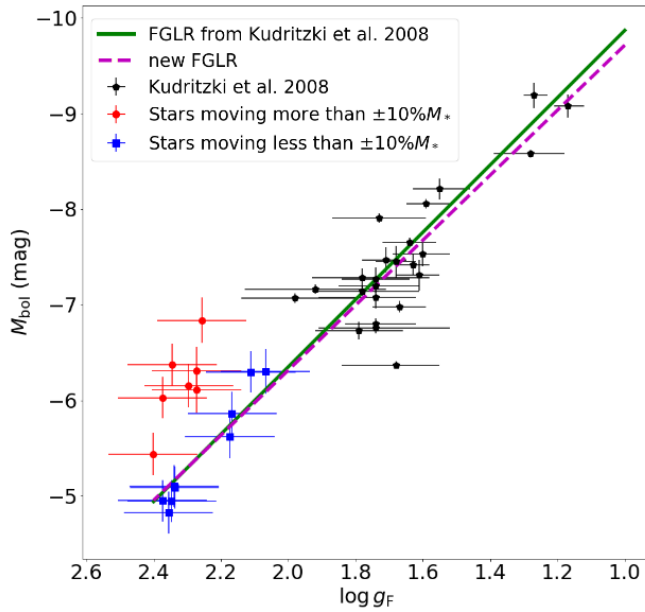


Figure 4: FGLR for the stars in NGC 300. The stars studied by Kudritzki et al. (2008) are shown in black pentagons, with the corresponding FGLR regression line marked in solid green. Blue squares and red circles mark the stars analysed in this work, with the magenta-dashed line representing the regression line derived from the black and blue symbols.

$a = -3.40 \pm 0.04$ and $b = 8.02 \pm 0.14$. The results from this work are also in accordance with the new FGLR distance to NGC 300 $(m - M)_{\text{FGLR}} = 26.34 \pm 0.06$ by Sextl et al. (2021).

3.1. Discrepant cases

As seen in Fig. 4, stars depicted by blue squares follow – within the uncertainties – the trend defined by the FGLR, while the ones represented by red dots deviate to some extent. For the stars depicted by red circles, either the derived luminosity is too high, or the flux-weighted gravity is too large (or both). The main reason for the luminosity (bolometric magnitude) to be too high would be for the apparent magnitude to be too high. This could mean that what is seen as a single star is a combination of several unresolved sources instead. Inspecting the MUSE datacube (see Fig. 1), none of these objects show signs of being an extended source, which makes it unlikely that they are large star clusters. On the other hand, it cannot be ruled out that they are small stellar aggregates that are not resolved at the distance of NGC 300.

An alternative explanation for this deviation could be the following: as we increase the $\log g_F$ and move to the bottom left of the FGLR, the stars decrease in mass. Population simulations predict that the FGLR will get wider for lower masses, as discussed by Meynet et al. (2015). Because of the so-called initial mass function (IMF) effect, we always expect to find a higher number of low mass stars than of massive stars (e.g. Salpeter 1955; Kroupa 2001), widening the FGLR because of the increased scatter.

4. Conclusions

We performed a quantitative spectroscopic analysis of 16 BA-type supergiants and bright giants in NGC 300, based on VLT/MUSE IFS data. Our focus lied on determining basic atmospheric and fundamental stellar parameters. This allowed us to extend the FGLR towards less luminous stars than studied before. However, the study has faced limitations by the relatively low $S/N \lesssim 20$ of the spectra. For future work, the S/N and spatial resolution should be improved by taking advantage of the adaptive optics mode of MUSE and longer exposure times. This would not only reduce the uncertainties for similar studies as this work, but would also help to determine metallicities and likely elemental abundances for selected individual chemical elements. Therefore, demonstrating the full potential of MUSE for extragalactic stellar astrophysics. In addition, BlueMUSE is the new proposed medium-resolution IFS instrument at the VLT. Optimized for the optical blue, BlueMUSE will be the perfect instrument to study hot massive stars as most of their spectral features are located in its spectral range - a Highlight Science Case outlined in the BlueMUSE White Paper (Richard et al. 2019).

References

- Baade, W. 1944, ApJ, 100, 137
 Bacon, R., et al. 2014, The Messenger, 157, 13
 Bresolin, F., Gieren, W., Kudritzki, R.-P., Pietrzyński, G., & Przybilla, N. 2002, ApJ, 567, 277
 Bresolin, F., Pietrzyński, G., Gieren, W., Kudritzki, R.-P., Przybilla, N., & Fouqué, P. 2004, ApJ, 600, 182
 Ekström, S., et al. 2012, A&A, 537, A146
 González-Torà, G., Urbaneja, M. A., Przybilla, N., Dreizler, S., Roth, M. M., Kamann, S., & Castro, N. 2022, A&A, 658, A117
 Hubble, E. P. 1929, ApJ, 69, 103
 Humphreys, R. M., & Aaronson, M. 1987, AJ, 94, 1156
 Humphreys, R. M., & Davidson, K. 1979, ApJ, 232, 409
 Kamann, S., Wisotzki, L., & Roth, M. M. 2013, A&A, 549, A71
 Kroupa, P. 2001, MNRAS, 322, 231
 Kudritzki, R. P., Bresolin, F., & Przybilla, N. 2003, ApJL, 582, L83
 Kudritzki, R. P., Urbaneja, M. A., Bresolin, F., Przybilla, N., Gieren, W., & Pietrzyński, G. 2008, ApJ, 681, 269
 Langer, N., & Kudritzki, R. P. 2014, A&A, 564, A52
 Meynet, G., Kudritzki, R. P., & Georgy, C. 2015, A&A, 581, A36
 Pietrzyński, G., Gieren, W., Fouqué, P., & Pont, F. 2001, A&A, 371, 497
 Przybilla, N., Butler, K., Becker, S. R., & Kudritzki, R. P. 2006, A&A, 445, 1099
 Richard, J., et al. 2019, arXiv e-prints, arXiv:1906.01657
 Rizzi, L., Bresolin, F., Kudritzki, R. P., Gieren, W., & Pietrzyński, G. 2006, ApJ, 638, 766
 Roth, M. M., et al. 2018, A&A, 618, A3 (Paper I)
 Salpeter, E. E. 1955, ApJ, 121, 161
 Sestl, E., Kudritzki, R.-P., Weller, J., Urbaneja, M. A., & Weiss, A. 2021, ApJ, 914, 94
 Urbaneja, M. A., et al. 2005, ApJ, 622, 862
 Weilbacher, P. M., et al. 2020, A&A, 641, A28

Discussion

QUESTION: How do you know that the stars are in the right evolutionary stage?

GONZÁLEZ-TORÀ: We plot all the targets both in the HRD and the sHRD. The blue dots in Figures 3a, 3b are the stars in the supergiant phase, since their photometric and spectroscopic information coincide (*see more in Section 3, 3rd and 4th paragraphs*).